Time-dependent quantum simulations of FH 2 – photoelectron spectra on new ab initio potential energy surfaces for the anionic and the neutral species

ARTICLE *in* CHEMICAL PHYSICS LETTERS · DECEMBER 1997

Impact Factor: 1.9 · DOI: 10.1016/S0009-2614(97)01209-8

2 AUTHORS:

Bernd Hartke
Christian-Albrechts-Universität zu Kiel
95 PUBLICATIONS **2,065** CITATIONS
SEE PROFILE

Hans-Joachim Werner
Universität Stuttgart
284 PUBLICATIONS **26,705** CITATIONS
SEE PROFILE

12 December 1997

ELSEVIER

Chemical Physics Letters 280 (1997) 430–438

CHEMICAL PHYSICS LETTERS

Time-dependent quantum simulations of FH_2^- photoelectron spectra on new ab initio potential energy surfaces for the anionic and the neutral species

Bernd Hartke, Hans-Joachim Werner

Institut für Theoretische Chemie, Universität Stuttgart, Pfaffenwaldring 55, D-70569 Stuttgart, Germany

Received 6 October 1997

Abstract

The photoelectron spectra ('transition state spectra') of FH_2^- generated experimentally from para- and normal-H_2 are simulated on new ab initio potential energy surfaces using standard quantum time-dependent wavepacket techniques, and compared directly to experimental spectra. Agreement between theory and experiment is improved compared to earlier simulations. Two factors are shown to contribute to this success: (1) the anharmonicity of the exact vibrational wavefunctions on a new ab initio surface for the anion and (2) a new spin–orbit correction applied to the ab initio surface for neutral FH_2. Possible reasons for the small remaining discrepancies are investigated and discussed. Finally, predictions are given for spectra obtainable in future high-resolution experiments of this system. © 1997 Elsevier Science B.V.

1. Introduction

The reaction $F + H_2 \rightarrow HF + H$ has become a textbook example [1] although its theoretical treatment proved to be challenging. Recently, however, theoretical and experimental results have advanced to a level of quantitative comparability [2–6]. A centerpiece of this development was the application of anion photoelectron spectroscopy [7] to the FH_2 system [8–10]. After earlier theoretical simulations of the spectra [10] using several different potential energy surfaces for neutral FH_2 had yielded results in strong qualitative disagreement with experiment, a new ab initio surface by Stark and Werner [2] (hereafter SW1) could be shown to reconcile theory and experiment for the first time [11]. In fact, the simulation was accurate enough to show that an earlier version of the para-H_2 experiment suffered from contamination by ortho-H_2. Later, Russell and Manolopoulos [12] were able to further improve the simulation by increasing the spectral energy resolution from 19 to 1 meV and by assigning all peaks in their high-resolution spectra.

Nevertheless, the older low-resolution results [11] still exhibited unexplained quantitative differences between experimental and theoretical spectra. In particular, the absolute energies of the peak positions were unknown and had to be fitted to experiment, and also the relative peak heights were not reproduced quite correctly. In the following, we will improve upon these defects by getting rid of two deficiencies of the theoretical treatment used so far [11,12]: (1) the assumption of a purely harmonic vibrational wavefunction [13] for FH_2^-, based on earlier ab initio results by Simons et al. [14]; and (2) the complete neglect of spin–orbit effects in the

PII S0009-2614(97)01209-8

neutral system. For item (1), we will use vibrational wavefunctions calculated on a new ab initio surface for the anionic species FH_2^- (hereafter SW). For item (2), we will employ a new spin–orbit corrected surface for FH_2 (hereafter HSW) [15]. Another related paper [6] will demonstrate the effect of the spin–orbit correction on quantum and quasiclassical reactive scattering results, both in the center-of-mass frame and in the laboratory frame.

This Letter is organized as follows: In Section 2, technical details are presented briefly. The new photoelectron spectra simulations are shown in Section 3, in direct comparison with earlier simulations and experimental results. The Letter ends with discussions and conclusions in Section 4.

2. Technical details

2.1. Potential energy surfaces

The HSW potential energy surface for the neutral system is based on the SW1 surface [2], with spin–orbit corrections added in the entrance channel. The spin–orbit (SO) matrix elements have been computed on the basis of the Breit–Pauli Hamiltonian using internally contracted multireference configuration interaction (MRCI) wavefunctions [16] for the lowest three electronic states, which correlate with the $F(^2P) + H_2$ asymptote. In a diabatic representation, as defined in Ref. [2], the SO matrix elements were found to be virtually independent of the bending angle γ and therefore it was sufficient to compute them for linear geometries. The angle-dependent adiabatic potential energy surfaces were obtained by diagonalizing the total Hamiltonian $H_{\mathrm{el}}^{\mathrm{dia}}(R,r,\gamma) + H_{\mathrm{SO}}^{\mathrm{dia}}(R,r)$ with the assumption that $H_{\mathrm{SO}}^{\mathrm{dia}}(R,r)$ is independent of γ (R is the distance between the F-atom and the H_2 center-of-mass, r the distance between the two H-atoms, and γ the angle between the corresponding vectors $\vec{R}$ and $\vec{r}$). The spin–orbit correction for the electronic ground state was spline fitted and then added to the SW1 potential energy fit [2]. The potential for the negative ion was computed with the same basis as the neutral surface (basis B of Ref. [2]) using singles and doubles coupled-cluster wavefunctions with perturbative corrections for triple excitations [CCSD(T)] [17]. About 500 points were computed on the potential energy surface and then fitted to an analytical function [18]. All ab initio calculations have been performed with the MOLPRO program [19]. A detailed description of both new potential energy surfaces and the fitting procedures will be given elsewhere [15].

2.2. Dynamical calculations

The simulations involve time-dependent split-operator propagations of FH_2^- vibrational functions on the neutral FH_2 potential energy surface.

In Refs. [11,12], a harmonic approximation to the para and ortho vibrational ground states of FH_2^- was used which is given by equation (5.5) in Zhang and Miller's paper [13]. Note, however, that in Refs. [11,12] as well as here the following parameters were used (in atomic units): $\alpha_R = 4.4252$, $\alpha_r = 17.3364$, $\alpha_\gamma = 6.5978$, $R_e = 3.921$, $r_e = 1.455$. These values are based on Simons et al.'s original data [14], with slight modifications. The values given in the paper by Zhang and Miller [13] are different, in particular the one for α_γ, possibly due to a misprint.

In contrast to Simons et al.'s ab initio data, the SW anion surface is a global one. This allows for accurate determination of FH_2^- bound states on this surface by standard procedures. We diagonalized the $J = 0$ Hamiltonian in the usual Jacobi coordinates with a distributed Gaussian [20–22] basis in R, particle-in-a-box functions in r and Legendre polynomials in γ, additionally employing an adiabatic reduction [20,21] of the basis in r and γ.

The converged eigenenergies of all bound states are given in Table 1. The notation used for classifying the states is this: n_R and n_γ give the number of nodes in the R- and γ-coordinates, respectively. p_γ is the symmetry (g = gerade/even, u = ungerade/odd) of the states with respect to the plane $\gamma = 90°$ in the double-minimum potential in the γ-coordinate. Note that the potential supports a considerable amount of R-excitation with bound character (corresponding to vibration of the F-atom relative to the H_2 moiety), but only at most one quantum of excitation in the γ-coordinate (hindered rotation of H_2). There is no bound state with excitation in the direction of the r-coordinate (vibration of the H_2 subunit). Of course, this simply reflects the degree of

Table 1
Energies and classification of the bound states of FH_2^-

No.	E^a (cm^{-1})	E^b (cm^{-1})	$n_R{}^c$	$n_\gamma{}^c$	$p_\gamma{}^c$
1	598.51	−1573.47	0	0	g
2	598.55	−1573.42	0	0	u
3	931.68	−1240.30	1	0	g
4	931.94	−1240.04	1	0	u
5	1210.00	−961.98	2	0	g
6	1210.84	−961.14	2	0	u
7	1444.12	−727.86	3	0	g
8	1446.12	−725.86	3	0	u
9	1643.29	−528.69	4	0	g
10	1647.50	−524.48	4	0	u
11	1811.82	−360.15	5	0	g
12	1820.51	−351.47	5	0	u
13	1930.35	−241.63	0	1	g
14	1949.31	−222.67	6	0	g
15	1967.00	−204.98	6	0	u
16	1994.69	−177.29	0	1	u
17	2052.44	−119.54	7	0	g
18	2086.80	−85.18	7	0	u
19	2089.09	−82.89	1	1	g
20	2119.38	−52.60	8	0	g
21	2154.49	−17.49	9	0	g

[a] Relative to the classical bottom of the $F^- + H_2$ asymptote.
[b] Relative to the asymptotic state $F^- + H_2(v = 0)$.
[c] See text for explanation of classification.

'softness' of the potential along these degrees of freedom. As a minor curiosity, note that all bound states have positive eigenenergies, with the bottom of the asymptotic $F^- + H_2$ valley taken as the zero of energy. That is, all these states are bound only due to the zero-point energy of H_2 in this asymptote, which is 6.210 kcal/mol ($= 2172$ cm^{-1}) on this surface.

Following Ref. [12], these bound eigenfunctions of the anion are then propagated in time on the potential energy surface for the neutral species. Possible contributions of transition moment functions are ignored (Condon approximation). The usual $J = 0$ Hamiltonian in Jacobi coordinates (without mass-scaling) is represented by the two-dimensional FFT method [23,24] in the R- and r-coordinates (78 grid points between $R = 0$ and 8.7 bohr, 65 grid points between $r = 0$ and 13.8 bohr) and a Legendre-DVR [25–29] in the γ-coordinate (with 77 points, after exploiting the permutation symmetry of the H_2 subunit). The standard split-operator method [30–32] is used for time propagation. Note that in this case it is not advisable to try the potentially more exact Chebyshev propagator [33], since the system can approach $R = 0$ on the neutral surface, for suitable values of γ. Via the $1/R^2$ characteristic of the rotational term in the Hamiltonian, this leads to an intolerable increase in the number of necessary Chebyshev expansion terms. Smooth but effective absorption of the wavepacket at the grid ends is achieved by the numerically optimized complex absorbing potentials constructed by Russell and Manolopoulos [12].

Spectra are obtained by a Fourier transform of the autocorrelation function. The technique closely follows the details given in Ref. [12]. The internal energy scale of the spectra is then transformed to the experimental kinetic energy scale of the photoelectrons via the energy conservation relation given in Ref. [11]. This relation involves the dissociation energy D_0 of the anion. In the case of Simons' anion, a value of 0.205 eV is used, which is known only inaccurately (± 0.1 eV) from the data of Simons et al., hence it is obtained by fitting the simulated spectra to experiment, as in Ref. [11].

In the case of the SW anion, we have calculated the value of D_0 from the SW ab initio surface to be 0.1938 eV ($D_e = 0.280$ eV). These simulations then yield absolute positions of the spectra, without the necessity of a fit by shifting them on the energy axis.

The finite energy resolution of the experiments is obtained in the simulation by damping the autocorrelation function with a suitable Gaussian [12]. For a resolution of 19 meV, therefore, relatively short propagation times on the order of 10000 atu (0.24 ps) are sufficient. This resolution is the one obtained in the experimental spectra by Neumark et al. [11]. A higher resolution of 1 meV requires propagations that are approximately ten times longer. This resolution will presumably be attainable with zero electron kinetic energy (ZEKE) techniques.

For brevity, only the para spectra will be discussed in detail. Some ortho and normal spectra (the latter being a 3:1 mixture of ortho and para results) will also be shown in the figures, for completeness. They reflect the same trends as the para spectra but are more congested and hence less easy to understand at first sight. All simulated spectra are scaled such that the height of the largest peak matches the

height of the corresponding peak in the experimental spectrum.

3. Photoelectron spectra of FH_2^-

3.1. Low-resolution spectra

Fig. 1a shows a direct comparison between experimental and simulated photo-electron spectra of para-FH_2^- at the experimental resolution of 19 meV. The simulation starts from Simons' anion and proceeds on the SW1 neutral surface; this corresponds to the results already published in Ref. [11]. The assignment given is that of Ref. [11], which was slightly corrected later [3].

Note that the nicely matched absolute peak positions are neither a surprise nor a true feature of the ab initio surfaces used since in this case they involve a fit via the D_0 parameter, as explained above.

Independent of this issue, relative peak positions and heights are reproduced tolerably well, in comparison with earlier simulation attempts [10,13], as noted in Ref. [11]. Quantitatively, however, some differences between theory and experiment are obvious: If one scaled the simulated spectrum such that the $(v = 0,\ j = 0)$ peak matches up with experiment, all $(v \geq 0,\ j > 0)$ peaks would be too small, in particular, the $(v = 1, j)$ group of peaks seems to be almost completely absent in the simulation.

It is tempting to assume that these defects are mainly due to the harmonic approximation of the anion wavefunction. Provided the given assignment is correct, it is likely that an anharmonic wavefunction will have a larger overlap with the excited $(v \geq 0,\ j > 0)$ resonance states near the barrier, leading to increased intensity of the corresponding peaks.

Therefore, we have substituted Simons' anion with exact vibrational anion wavefunctions, calculated on the new SW anion surface: $v = 0,\ j = 0$ for the para case and $v = 0,\ j = 1$ for the ortho case. Propagation of the para function on the SW1 surface, i.e. still without employing the spin–orbit corrected HSW surface, yields the spectrum depicted in Fig. 1b, again in direct comparison with experiment.

The relative peak height $(v = 0,\ j = 0)/(v = 0,\ j = 2)$ is now exactly on target. The higher-j peaks $(v = 0,\ j = 4)$ and $(v = 0,\ j = 6)$ have notably grown

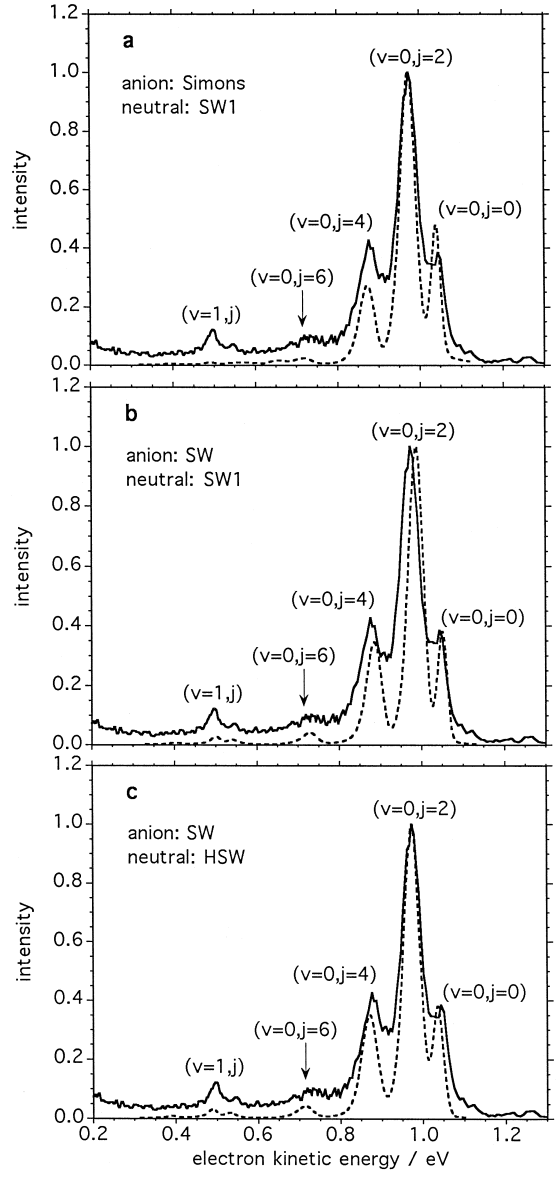

Fig. 1. Experimental para-FH_2^- photoelectron spectra (solid line in each panel) vs. different simulations (dashed lines): (a) Simons' anion propagated on the SW1 surface; (b) anharmonic anion function calculated on the SW surface and propagated on the SW1 surface; (c) same anion function as in (b), but propagated on the HSW surface. All spectra are given on the experimental electron kinetic energy scale in eV and have an experimental energy resolution of 19 meV. Intensities are in arbitrary units, with a value of 1 assigned to the largest peak.

and the peak group $(v = 1, j)$ has appeared in the simulation, at approximately the correct position — all of this in accord with the above simple expectation. However, the peaks $(v = 0,\ j = 4)$, $(v = 0,\ j = 6)$ and $(v = 1, j)$ are still somewhat too small and, most glaringly, the peak positions, which are now absolute and not adjusted anymore, turn out to be wrong. (The normal case, not shown, gives exactly the same trends.) The shift of the theoretical peak positions to higher electron kinetic energy indicates that either the barrier height on the neutral surface is too low, or D_0 of the anion is too small.

Interestingly, the wrong peak positions are remedied when we now further modify the simulation by making the transition from the SW1 neutral surface to HSW, i.e. by adding in the spin–orbit correction, see Fig. 1c. The main effect of this change is a shift of the whole spectrum on the energy scale, and this brings the absolute position of the largest peak $(v = 0,\ j = 2)$ back to exactly the correct position! This is brilliant, considering that we do not have any free parameters available for fitting the peak positions anymore. Unfortunately, this shift does not really improve the positions of the other peaks. (Again, the effect on the normal case is completely analogous.) It should be mentioned, however, that there could be a fortuitous error compensation of the barrier height of the neutral surface and the dissociation energy of the anion; this cannot be ruled out by the present simulations.

Other effects of the spin–orbit correction are barely visible on the scale chosen here. This is not surprising, since the shape of the neutral potential energy surface in the vicinity of the transition state is hardly changed by the spin–orbit coupling [2,15]. Thus, the energy shift of the spectrum should correspond closely to the asymptotic energy shift of the $F(^2P_{3/2})$ state relative to the average energy of the fluorine spin–orbit states, i.e. $\frac{1}{3}(E(^2P_{1/2}) - E^2P_{3/2}))$ $= 0.385$ kcal/mol $(= 0.0167$ eV). From the simulated spectral data, the actual shift is $\sim \frac{2}{3}$ of this value; the remainder corresponds to changes in peak shape, which in turn are caused by the minor potential shape changes induced by the not entirely 'flat' shape of the spin–orbit correction [15].

The absence of further large changes besides this overall shift, however, means that the other defects noted in the previous case also are present here, in particular, the peaks $(v = 0,\ j = 4)$, $(v = 0,\ j = 6)$ and $(v = 1, j)$ are again somewhat too small. Since these differences appear in the peaks corresponding to (v, j)-excited resonance functions at the transition state, one may be tempted to speculate that vibrationally excited anion wavefunctions could lead to larger overlaps with these resonance functions, i.e. that raising the temperature above 0 K in the simulation could improve the agreement. This hypothesis is easily checked, since we have a full FH_2^- surface available, allowing for the calculation of all vibrationally excited bound states of the anion. As an example, Fig. 2a shows the spectrum arising from bound anion functions with one quantum added in the R-degree of freedom (function No. 3 with the designation $(1, 0, g)$ in Table 1). Clearly, admixture of this spectrum via a Boltzmann weighting will not improve agreement with experiment; in fact, it will make it worse. This is borne out by Fig. 2b and c, giving the full temperature dependence of the para and normal spectra, by an appropriate Boltzmann weighting of all bound states of FH_2^- that contribute significantly. At $T < 100$ K, the temperature dependence is below graphical resolution. Significant changes grow in only at room temperature or above. But even in the unlikely case that the experiments actually have accessed such a temperature regime, the changes in the simulated spectra would lead away from the given experimental spectra rather than towards them, as evidenced by the simulations at $T = 500$ K.

Actually, the spectra of the excited states, e.g. the one shown in Fig. 2a, have a somewhat unexpected appearance, in particular, their peak positions do not line up with the peak positions of the ground spectra. This seems to be impossible, since the peak positions are interpreted to be a direct reflection of resonance energies on the neutral surface, and these are surely not going to change with temperature. However, this seeming paradox can be explained by looking at the spectra in higher resolution.

3.2. High-resolution spectra

Fig. 3a and b displays the para spectra in 1.0 meV resolution, for Simons' anion propagated on SW1 and the SW anion propagated on HSW, respectively. Fig. 3c gives the ortho case for the SW anion

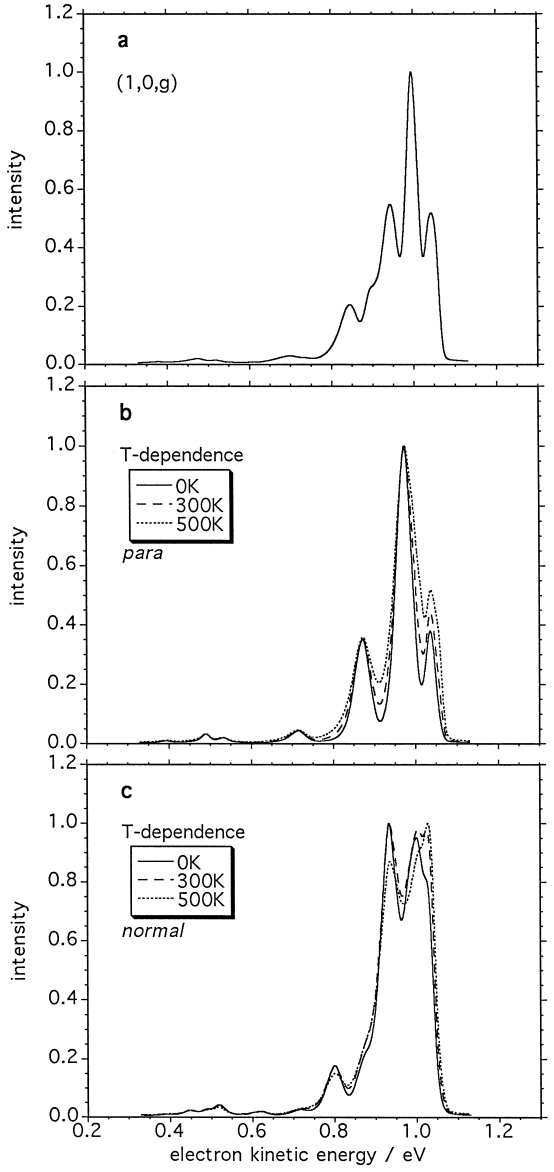

Fig. 2. Simulated spectra at 19 meV resolution, starting from anharmonic anion functions calculated on the SW surface and propagated on the HSW surface. In panel (a), the vibrational para anion eigenfunction No. 3 of Table 1 was used. Panels (b) and (c) show sums of spectra arising from Boltzmann distributions of the bound anion states, corresponding to temperatures of 0 K (solid line), 300 K (dashed line), and 500 K (dotted line), for the para case (b) and the normal case (c). In order to facilitate comparisons of panels (a) and (b) with Fig. 1, the energy range and scale is the same as in Fig. 1.

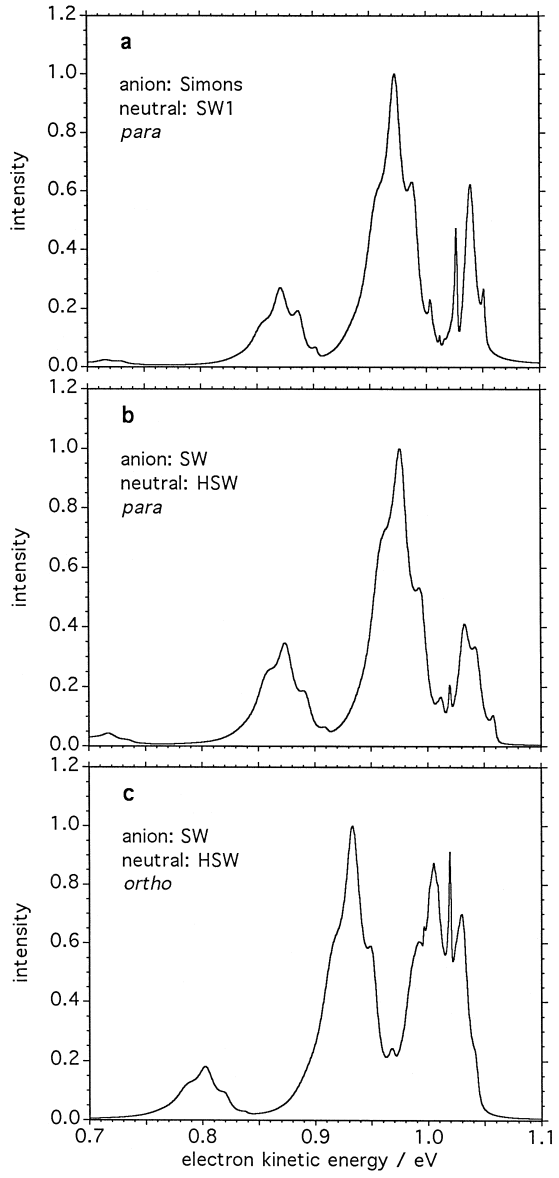

Fig. 3. Simulated spectra at 1 meV resolution: (a) Simons' para anion function propagated on the SW1 surface, (b) lowest para and (c) lowest ortho function of the SW anion surface propagated on the HSW surface. In order not to obscure the fine structure, only the energy range corresponding to the strongest peaks in low resolution is shown.

propagated on HSW, for completeness (the normal spectrum is a 3:1 mixture of Fig. 3b and c). Fig. 3a corresponds to the result already published by Russell and Manolopoulos [12]. In that work, a complete

assignment of all peaks was established (cf. table 1 of Ref. [12]). From this assignment, it is obvious that the sharp peaks correspond to long-lived resonances associated with the Van der Waals wells in the entrance and exit valleys, while the broader peaks are related to direct scattering resonances. The nodal structures of the latter can be characterized by the low-resolution assignment given above (which is thus superseded by the more exact assignment by Russell and Manolopoulos [12]).

Direct comparison between the (Simons, SW1) and (HSW, SW) cases in Fig. 3a and b shows that the sharp peaks due to the Van der Waals resonances are much smaller in the second case. A simple explanation for this could be the increased barrier height on HSW: it imparts more kinetic energy on the initial wavepacket, such that trapping in the Van der Waals wells becomes less pronounced.

By comparing high-resolution spectra of excited anion states, for example the one with one quantum of excitation in the R-coordinate, the $(1, 0, g)$ state (cf. Fig. 4a), with the high-resolution spectrum of the ground state (Fig. 3b), one can see immediately that all peaks do line up exactly, as expected. But, of course, the intensity pattern is changed substantially, and this leads to the above-mentioned seeming paradox of 'shifted' peaks in low resolution. Actually, in low resolution, the peaks are mixed peaks and the assignment given is only an approximate one. When changing the initial state wavefunction, the peak character in the low-resolution spectrum changes, and this just looks like a shift.

In Fig. 4b and c, the temperature dependence of the high-resolution para and normal spectra is demonstrated, in analogy to Fig. 2b and c. They reveal that at high temperatures the sharp resonance peaks in the region between 1.0 and 1.1 eV electron kinetic energy, which were getting smaller upon switching from (Simons, SW1) to (SW, HSW) (Fig. 3a and b) are growing again. This could provide interesting avenues for experiment, provided this temperature region can be accessed.

As an aside, in Ref. [3] it was mentioned that the first peaks of the low-resolution para and ortho spectra are curiously close to each other, and that this is a weak point of the whole peak assignment argumentation. In Ref. [12], it is confirmed that the two high-resolution peaks of para ($v = 0,\ j = 0$) and ortho ($v = 0,\ j = 1$) are just 0.003 eV apart, but this is not discussed. However, the explanation is fairly obvious: Examination of the potential energy surface in the transition state region in (R, γ), cf. fig. 1 of Ref. [11] shows that a (curved) one-dimensional cut

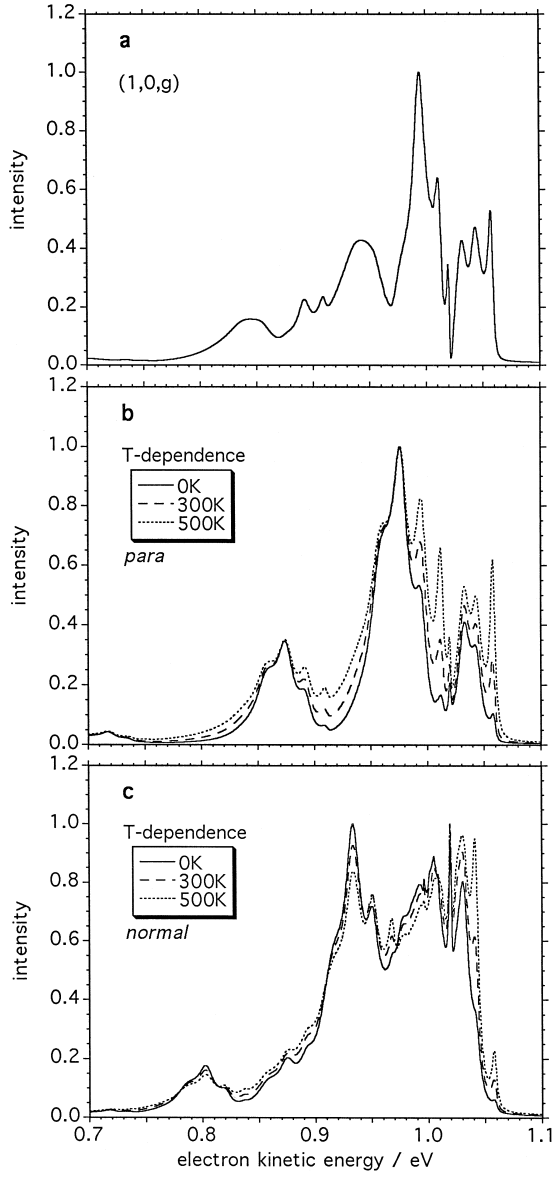

Fig. 4. Simulated spectra at 1 meV resolution: This figure is the high-resolution version of Fig. 2. Note, however, that the energy scale is the same as in Fig. 3, for better comparison and clarity. The $T = 0$ K normal spectrum in panel (c) is identical to a 3:1 mixture of Fig. 3c (ortho) and Fig. 3b (para).

approximately perpendicular to the reaction path through the transition state clearly has a double-minimum character. So, the lowest two states (belonging to para and ortho by symmetry) are below the double-minimum barrier and separated only by a small tunneling splitting, while the higher states are above the barrier and form a nice regular (hindered-)rotor pattern.

The high-resolution spectra given here constitute a prediction for the result of the actual high-resolution experiment the group of Neumark is planning to make. Since the positions of all resonance peaks depend strongly on small features of the neutral potential energy surface, this is going to be a stringent test for this surface.

4. Discussion and conclusions

While we have to wait for the results of the high-resolution experiment, we can already draw conclusions from the comparison of the low-resolution simulations to experiment: As demonstrated above, the SW anion surface significantly improves the relative peak heights in the simulated spectra and brings them into very good quantitative agreement with experiment. The spin–orbit correction to the neutral surface, incorporated into HSW, is vitally necessary to bring the peaks in the photoelectron spectra to the correct absolute positions. This is quite remarkable, since the spin–orbit correction is relativistic but FH_2 clearly is not a heavy system.

Some quantitative discrepancies between theory and experiment are still remaining. In particular, the relative peak heights of the peaks $(v = 0,\ j \geq 4)$ and $(v = 1, j)$ are too small, and several peak positions are slightly wrong.

Let us examine several possible sources of error in the theoretical simulations in turn: obviously, defects in the two ab initio surfaces involved (anion and neutral) cannot be ruled out completely, even though quite careful tests of basis set convergence and correlation treatment have been performed [2,15]. The weakest part of the ab initio calculations for the neutral surface is probably the fact that the Davidson correction for higher excitations leads to a substantial reduction of the barrier height and also to some change of the shape of the potential energy surface. The excellent agreement of the Davidson corrected MRCI barrier height with the full CI (FCI) result for a smaller basis set [34] is certainly somewhat fortuitous, and it is unknown how well the FCI result would be reproduced with a large basis set. Furthermore, local deviations between the ab initio points and the fit in dynamically relevant regions may still be present.

Other sources of error also appear to be likely: Following common practice in simulations of this type (with a few notable exceptions, e.g. Refs. [35,36]), we have employed the $J = 0$ approximation; this is tolerable as long as vibration–rotation coupling is not too strong. Similarly, the Condon approximation was applied by ignoring dipole transition moments. Both approximations are probably not overwhelmingly good, in view of the fact that the anion ground state is linear while the barrier on the neutral surface is with 61°, clearly bent (however, it is only 0.39 kcal/mol lower than the linear barrier). Finally, as in the reactive scattering calculations presented in Ref. [6], the assumption of a single adiabatic Born–Oppenheimer surface is a severe approximation, due to the presence of a conical intersection of the lowest two spin–orbit states between the barrier and the Van der Waals well in the entrance channel. However, since the initial wavepacket is so close to the barrier itself, the importance of this approximation is presumably larger in reactive scattering.

While the spin–orbit correction appears to be a necessary step of improvement in this Letter, the reactive scattering results presented elsewhere [6] show that HSW is not convincingly better than SW1 and definitely not the ultimate surface. Since the largest remaining possible source of error in those scattering calculations is the assumption of a single Born–Oppenheimer surface, the next step definitely has to be the elimination of this assumption by a multi-surface treatment. This will be addressed by future work.

Acknowledgements

BH would like to thank Heiner Flöthmann, Reinhard Schinke, Caroline Russell and David Manolopoulos for many helpful hints and discus-

sions regarding time-dependent propagation techniques and their applications. This work was generously supported by the Deutsche Forschungsgemeinschaft in the Schwerpunktprogramm 'Zeitabhängige Phänomene und Methoden in Quantensystemen der Physik und Chemie', the Fonds der Chemischen Industrie, and the European Training and Mobility Research Network FMRX-CT96-0088.

References

[1] R.D. Levine, R.B. Bernstein, Molecular Reaction Dynamics and Chemical Reactivity, Oxford University Press, New York, 1987.
[2] K. Stark, H.-J. Werner, J. Chem. Phys. 104 (1996) 6515.
[3] J.F. Castillo, D.E. Manolopoulos, K. Stark, H.-J. Werner, J. Chem. Phys. 104 (1996) 6531.
[4] D.E. Manolopoulos, J. Chem. Soc., Faraday Trans. 93 (1997) 673.
[5] F.J. Aoiz, L. Bañares, B. Martínez-Haya, J.F. Castillo, D.E. Manolopoulos, K. Stark, H.-J. Werner, J. Phys. Chem. A 101 (1997) 6403.
[6] B. Hartke, K. Stark, H.-J. Werner, J.F. Castillo, D.E. Manolopoulos, L. Bañares, B. Martínez-Haya, F.J. Aoiz (in preparation).
[7] R.B. Metz, S.E. Bradforth, D.M. Neumark, Adv. Chem. Phys. 81 (1992) 1.
[8] A. Weaver, R.B. Metz, S.E. Bradforth, D.M. Neumark, J. Chem. Phys. 93 (1990) 5352.
[9] A. Weaver, D.M. Neumark, Faraday Discuss. Chem. Soc. 91 (1991) 5.
[10] S.E. Bradforth, D.W. Arnold, D.M. Neumark, D.E. Manolopoulos, J. Chem. Phys. 99 (1993) 6345.
[11] D.E. Manolopoulos, K. Stark, H.-J. Werner, D.W. Arnold, S.E. Bradforth, D.M. Neumark, Science 262 (1993) 1852.
[12] C.L. Russell, D.E. Manolopoulos, Chem. Phys. Lett. 256 (1996) 465.
[13] J.Z.H. Zhang, W.H. Miller, J. Chem. Phys. 92 (1990) 1811.
[14] J.A. Nichols, R.A. Kendall, S.J. Cole, J. Simons, J. Phys. Chem. 95 (1991) 1074.
[15] B. Hartke, K. Stark, H.-J. Werner (in preparation).
[16] H.-J. Werner, P.J. Knowles, J. Chem. Phys. 89 (1988) 5803.
[17] C. Hampel, K.A. Peterson, H.-J. Werner, Chem. Phys. Lett. 190 (1992) 1, and references therein.
[18] K. Stark, Dissertation, University of Stuttgart, Stuttgart, 1996.
[19] MOLPRO is a package of ab initio programs written by H.-J. Werner, P.J. Knowles, with contributions from R.D. Amos, A. Berning, D.L. Cooper, M.J.O. Deegan, A.J. Dobbyn, F. Eckert, C. Hampel, T. Leininger, R. Lindh, A.W. Lloyd, W. Meyer, M.E. Mura, A. Nicklass, P. Palmieri, K. Peterson, R. Pitzer, P. Pulay, G. Rauhut, M. Schütz, H. Stoll, A.J. Stone, T. Thorsteinsson.
[20] Z. Bačić, J.C. Light, J. Chem. Phys. 85 (1986) 4594.
[21] Z. Bačić, J.C. Light, J. Chem. Phys. 87 (1987) 4008.
[22] I.P. Hamilton, J.C. Light, J. Chem. Phys. 84 (1986) 306.
[23] D. Kosloff, R. Kosloff, J. Comput. Phys. 52 (1983) 35.
[24] R. Kosloff, J. Phys. Chem. 92 (1988) 2087.
[25] J.C. Light, I.P. Hamilton, J.V. Lill, J. Chem. Phys. 82 (1985) 1400.
[26] J.P. Hamilton, J.C. Light, J. Chem. Phys. 84 (1986) 306.
[27] S.E. Choi, J.C. Light, J. Chem. Phys. 90 (1989) 2593.
[28] Z. Bačić, J.C. Light, Annu. Rev. Phys. Chem. 40 (1989) 469.
[29] M.R. Hermann, J.A. Fleck Jr., Phys. Rev. A 38 (1988) 6000.
[30] J.A. Fleck Jr., J.R Morris, M.D. Feit, Appl. Phys. 10 (1976) 129.
[31] M.D. Feit, J.A. Fleck Jr., A. Steiger, J. Comput. Phys. 47 (1982) 412.
[32] C. Leforestier, R.H. Bisseling, C. Cerjan, M.D. Feit, R. Friesner, A. Guldberg, A. Hammerich, G. Jolicard, W. Karrlein, H.-D. Meyer, N. Lipkin, O. Roncero, R. Kosloff, J. Comput. Phys. 94 (1991) 59.
[33] H. Tal-Ezer, R. Kosloff, J. Chem. Phys. 81 (1984) 3722.
[34] P.J. Knowles, K. Stark, H.-J. Werner, Chem. Phys. Lett. 185 (1991) 555.
[35] J.M. Bowman, R.C. Mayrhofer, Y. Amatatsu, J. Chem. Phys. 101 (1994) 9469.
[36] H. Wei, T. Carrington Jr., J. Chem. Phys. 105 (1996) 141.